

Supporting information for

**Theoretical and experimental studies of high efficient all-solid Z-scheme TiO₂-
TiC/g-C₃N₄ for photocatalytic CO₂ reduction via dry reforming of methane**

Ziyi Li, Yu Mao*, Yufei Huang, Ding Wei, Ming Chen, Yangqiang Huang, Bo Jin,
Xiao Luo*, Zhiwu Liang*

Joint International Center for CO₂ Capture and Storage (iCCS), Provincial Hunan Key
Laboratory for Cost-effective Utilization of Fossil Fuel Aimed at Reducing Carbon-
dioxide Emissions, College of Chemistry and Chemical Engineering, The Engineering
Research Center of Advanced Catalysis, Ministry of Education, Hunan University,
Changsha 410082, P. R. China

***CORRESPONDING AUTHORS:**

1. Dr. Yu Mao

Tel.: +86-18216010211;

Email address: yumao@hnu.edu.cn

2. Dr. Xiao Luo

Tel.: +86-18627329998;

Email address: x_luo@hnu.edu.cn

3. Dr. Zhiwu Liang

Tel.: +86-13618481627; fax: +86-731-88573033;

E-mail address: zwliang@hnu.edu.cn

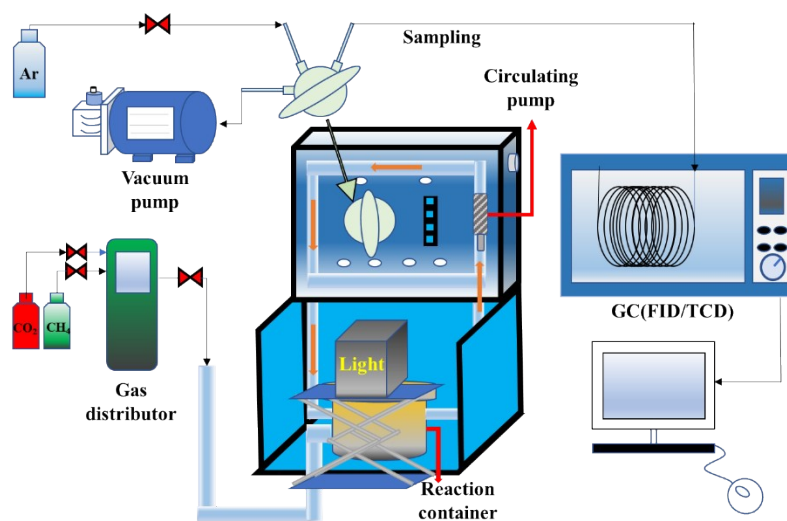


Figure S1. The diagram of the experimental device for photocatalytic CO₂ in the presence of CH₄.

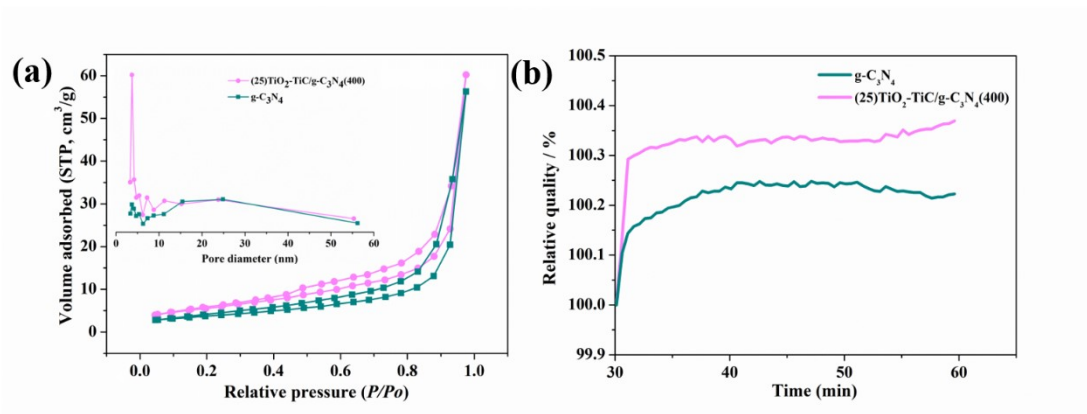


Figure S2. (a) N₂ physisorption isotherms and corresponding pore size distribution curves (inset) and (b) The CO₂ adsorption capacity of g-C₃N₄ and (25)TiO₂-TiC/g-C₃N₄(400).

Table S1. BET specific surface area and total pore volume of g-C₃N₄ and (25)TiO₂-TiC/g-C₃N₄(400).

Parameter	g-C ₃ N ₄	(25)TiO ₂ -TiC/g-C ₃ N ₄ (400)
Specific surface area (m ² /g)	16.920	21.503
Total pore volume (cm ³ /g)	0.087	0.078

Table S2. Factors and levels of the orthogonal test.

	Level 1	Level 2	Level 3	Level 4
F _A : Absolute pressure (kPa)	10	20	30	40
F _B : CH ₄ to CO ₂ ratio	2:1	1:1	1:2	1:3
F _C : TiC loading (mg)	15	20	25	30
F _D : Calcination temperature (°C)	350	400	450	500

Table S3. The detailed experimental conditions of four factors and four levels ($L_{16}(4^4)$) orthogonal test.

Experiment Numbers	F _A : pressure (kPa)	F _B : mole ratio of CH ₄ : CO ₂	F _C : Loading of TiC (mg)	F _D : calcination temperature (°C)
1	10	2:1	15	350
2	10	1:1	20	400
3	10	1:2	25	450
4	10	1:3	30	500
5	20	2:1	20	450
6	20	1:1	15	500
7	20	1:2	30	350
8	20	1:3	25	400
9	30	2:1	25	500
10	30	1:1	30	450
11	30	1:2	15	400
12	30	1:3	20	350
13	40	2:1	30	400
14	40	1:1	25	350
15	40	1:2	20	500
16	40	1:3	15	450

Table S4. The experimental results of orthogonal test (L₁₆(4⁴)).

Experiment Numbers	H ₂ (μmol)	CO (μmol)	TOF _{H2} (μmol g ⁻¹ h ⁻¹)	TOF _{CO} (μmol g ⁻¹ h ⁻¹)	Conversion rates of CH ₄ (%)
1	0.21	0.56	1.07	2.8	1.8
2	0.38	1.39	1.91	6.95	1.584
3	0.21	1.18	1.05	5.91	0.6
4	0.20	0.70	1.00	3.49	3.29
5	0.34	1.04	1.71	5.22	1.53
6	0.36	0.57	1.79	2.83	1.58
7	0.39	0.81	1.96	4.06	1.12
8	0.19	1.65	0.93	8.27	1.46
9	0.40	1.50	1.99	7.52	2.89
10	0.23	0.86	1.14	4.28	1.22
11	0.21	2.16	1.04	10.78	1.373
12	0.40	1.33	1.98	6.24	1.23
13	0.36	2.03	1.79	10.17	3.43
14	0.29	1.22	1.45	6.11	0.66
15	0.17	1.15	0.87	5.74	1.08
16	0.27	1.38	1.34	6.89	1.01

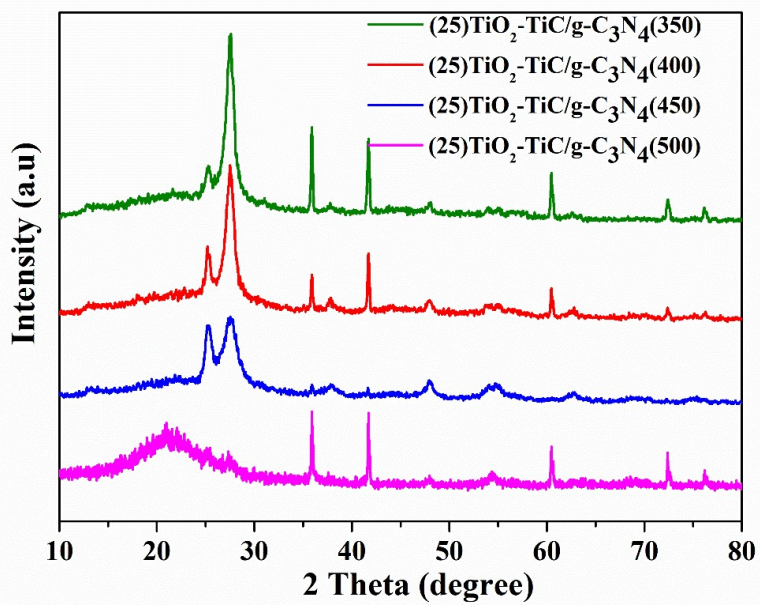


Figure S3. X-ray diffraction patterns of (25)TiO₂-TiC/g-C₃N₄(350), (25)TiO₂-TiC/g-C₃N₄(400), (25)TiO₂-TiC/g-C₃N₄(450), (25)TiO₂-TiC/g-C₃N₄(500).

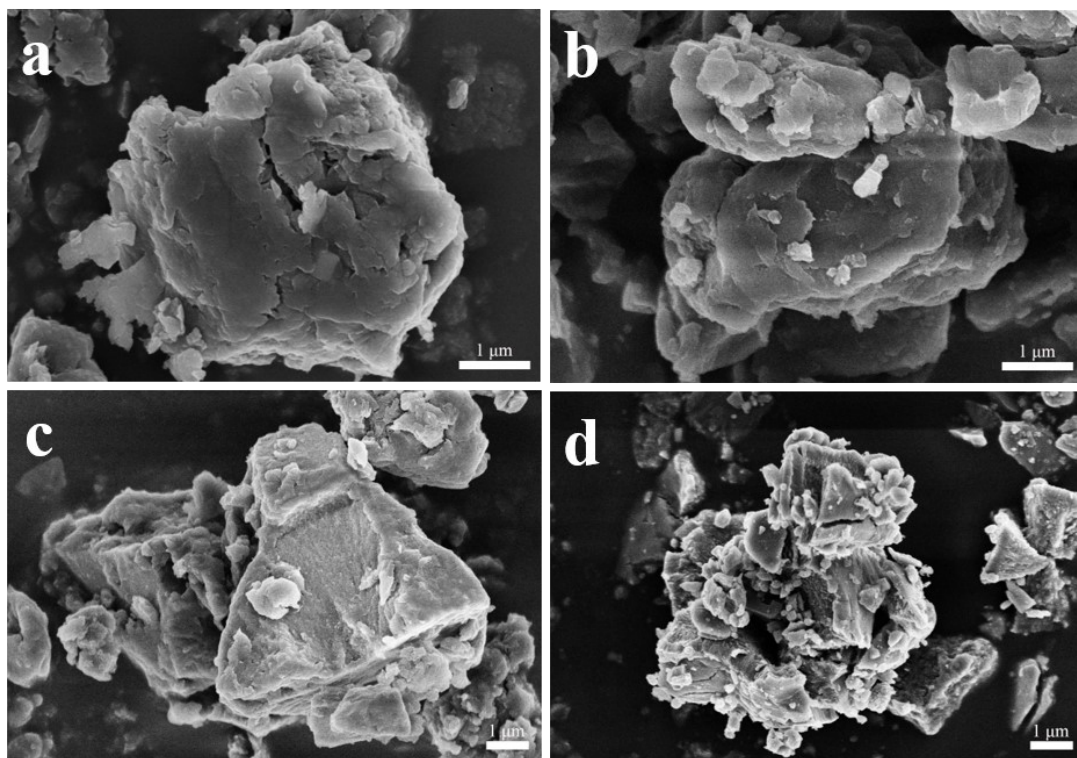


Figure S4. SEM patterns of (25)TiO₂-TiC/g-C₃N₄(350), (25)TiO₂-TiC/g-C₃N₄(400), (25)TiO₂-TiC/g-C₃N₄(450), (25)TiO₂-TiC/g-C₃N₄(500).

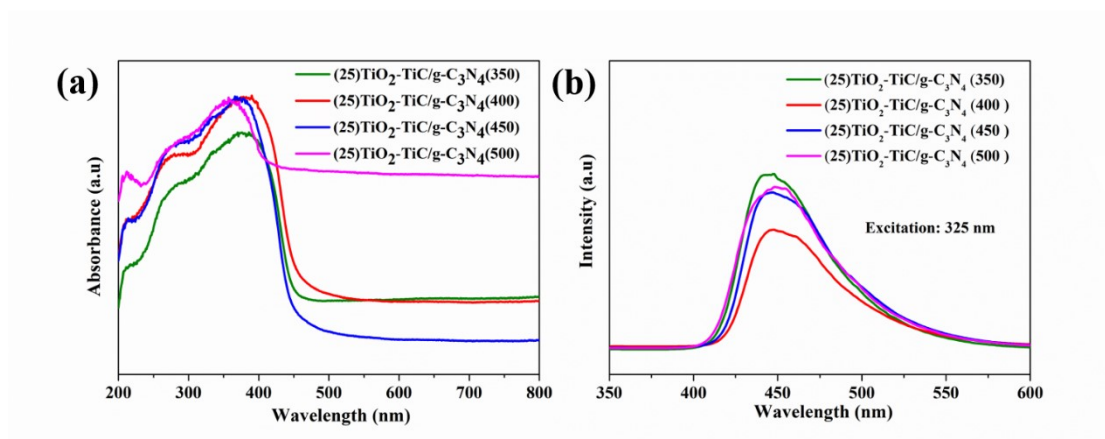


Figure S5. (a)UV-vis absorption spectra and (b) PL emission spectra of $\text{TiO}_2\text{-TiC/g-C}_3\text{N}_4$ calcinating under different temperature.

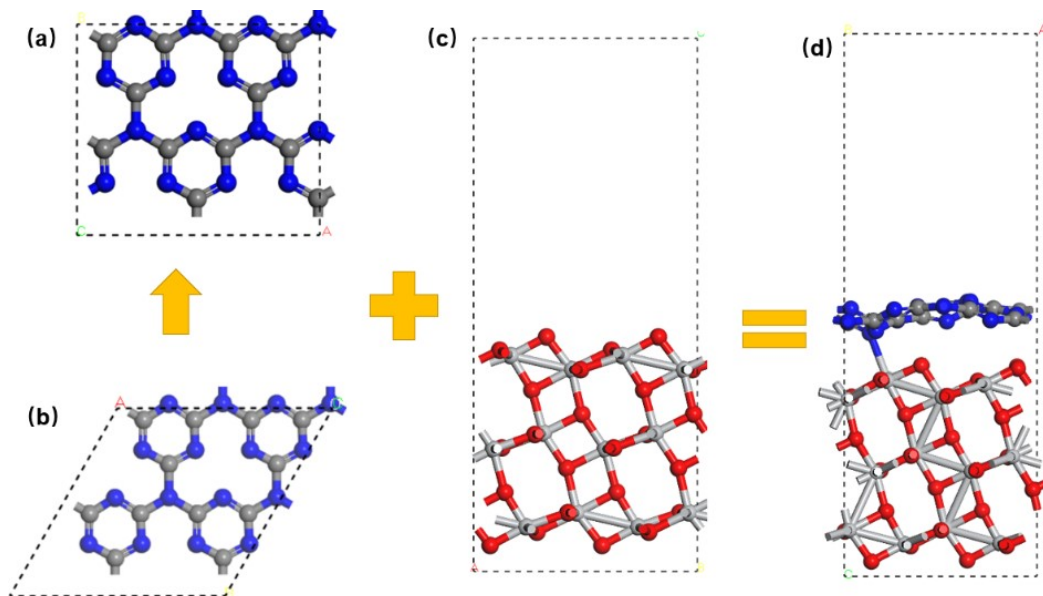


Figure S6. Illustrations of (a) $2 \times \sqrt{3}$ relaxed rectangular $\text{g-C}_3\text{N}_4$ monolayer; (b) original $\text{g-C}_3\text{N}_4$ monolayer; (c) TiO_2 (101) surface; (d) $\text{TiO}_2/\text{g-C}_3\text{N}_4$ heterostructure. Deep gray, blue, red, and light gray balls represent C, N, O and Ti atoms, respectively; this notation is used throughout the paper.

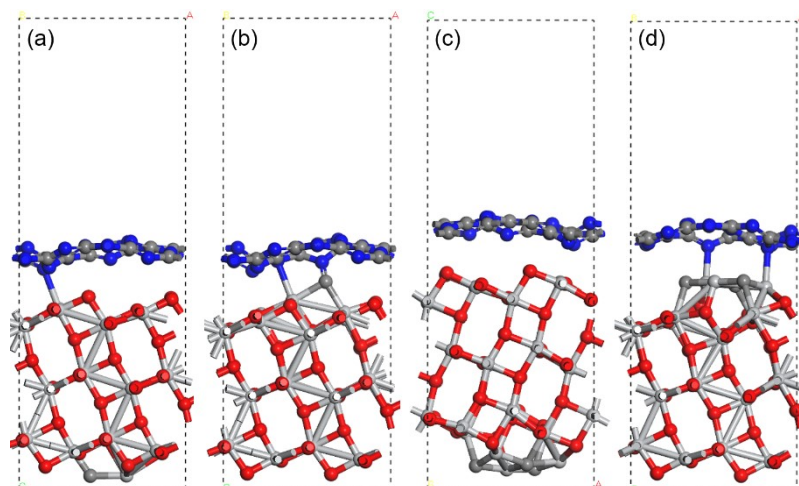


Figure S7. Illustrations of (a) $\text{TiO}_2\text{-TiC/g-C}_3\text{N}_4$ heterostructure with TiC on the TiO_2 side; (b) $\text{TiO}_2\text{-TiC/g-C}_3\text{N}_4$ heterostructure with TiC between TiO_2 and $\text{g-C}_3\text{N}_4$; (c) $\text{TiO}_2\text{-TiC/g-C}_3\text{N}_4$ heterostructure with $(\text{TiC})_3$ on the TiO_2 side; (d) $\text{TiO}_2\text{-TiC/g-C}_3\text{N}_4$ heterostructure with $(\text{TiC})_3$ between TiO_2 and $\text{g-C}_3\text{N}_4$.

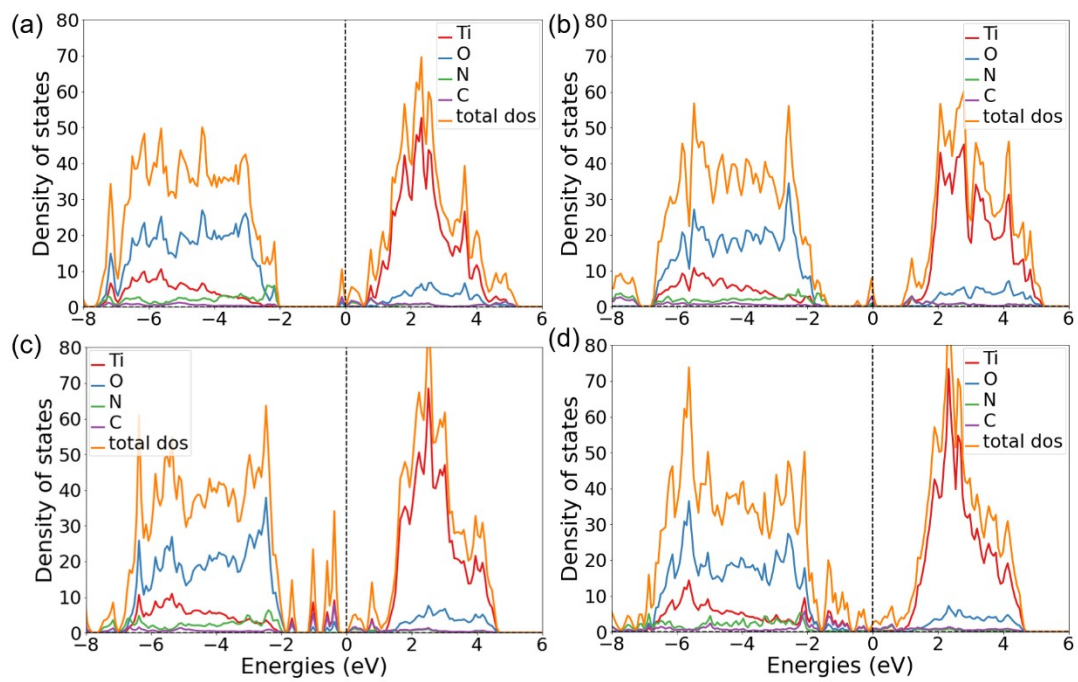


Figure S8. Density of state (DOS) of four structures in Figure S7. (a) – (d) correspond to structures (a) – (d) in Figure S7.

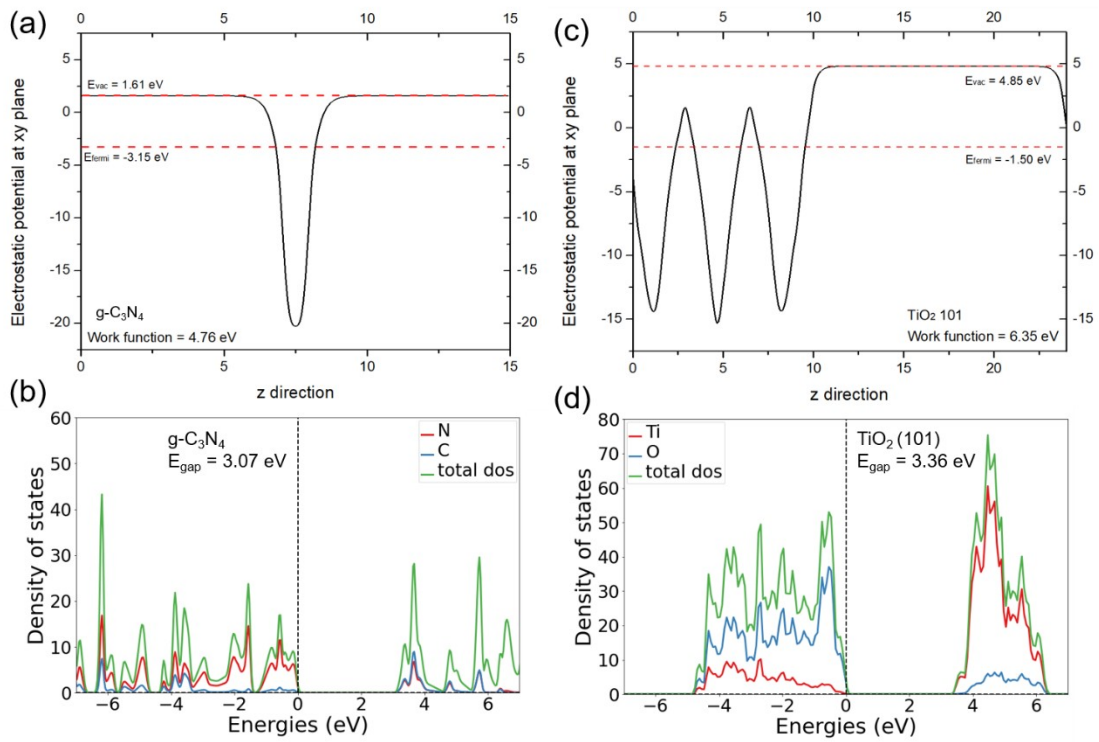


Figure S9. Electrostatic potentials and density of states of (ab) the monolayer $g\text{-C}_3\text{N}_4$; (cd) $\text{TiO}_2(101)$ surface. The DOS Figures in this study are plotted using DosPlotter module in Pymatgen python package (<https://pymatgen.org/>).

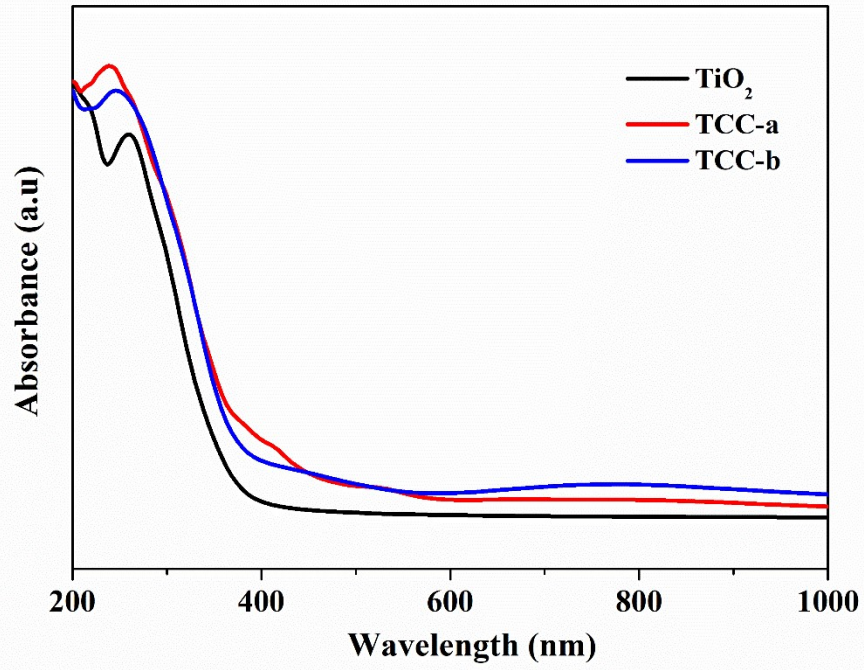


Figure S10. Calculated optical adsorption spectra of TiO₂(101), TCC-a, and TCC-b.